

Constructive Interference Between Disordered Couplings Enhances Multiparty Entanglement in Quantum Heisenberg Spin Glass Models

Utkarsh Mishra, Debraj Rakshit, R. Prabhu, Aditi Sen(De) and Ujjwal Sen
Harish-Chandra Research Institute, Chhatnag Road, Jhansi, Allahabad 211 019, India

We probe one-dimensional arrays of quantum spin-1/2 particles, governed by the Heisenberg spin glass Hamiltonian with natural or engineered quenched disordered couplings in an external magnetic field. We find that these systems allow the order from disorder phenomenon – disorder-induced enhancement – for magnetization, classical correlators, and bipartite as well as multipartite entanglement, wherein a disordered system has a higher value of the quenched averaged physical observable than in the corresponding ordered system. Moreover, the system also harbors parameter ranges where simultaneous application of independent quenched disorders results in order from disorder, while the same is absent with individual application of the same disorders – we term the phenomenon as constructive interference and the corresponding parameter stretches as the Venus regions. Interestingly, constructive interference has only been observed for multiparty entanglement and is absent for the single- and two-party observables.

I. INTRODUCTION

Research in implementation of quantum devices has led to the identification of useful multiparty quantum information processing tasks, like quantum secret sharing [1], cluster state quantum computation [2], quantum state transmission [3], and distributed quantum dense coding [4]. These multisite tasks have already been implemented in several physical systems like ion-traps [5], photons [6], optical lattices [7], and superconducting qubits [8]. It is widely believed that understanding the role of bipartite and multipartite entanglement [9] in these protocols in particular and quantum many-body systems in general, is crucial to gain the ability to build scalable decoherence-resistant efficient quantum devices. The wide interest in such activities is also due to the fact that several concepts developed in quantum information science turn out to be useful tools to detect co-operative phenomena [10–12], like quantum phase transitions and thermal transitions, and can help to develop approximate methods to obtain the ground states of non-integrable systems [13].

The importance of studying the effect of disorder in many-body systems can hardly be overestimated [14–17]. Realization of most physical systems inherently results in impurities or defects. Moreover, disordered systems, both classical and quantum, display counterintuitive phenomena like disorder-induced order or order from disorder in several physical quantities like magnetization, classical correlators, and entanglement [17–19]. At the same time, disordered systems sustain rich phases like spin glass [20] and Bose glass [21], and phenomena like Anderson localization [22] and high T_c -superconductivity [23]. Recent experimental developments, especially in ultra-cold gases, give rise to the possibility of introducing disorder in a controlled way [24] and hence paves the way for novel recipes of observation of these properties in the laboratory.

In this paper, we concentrate on the behavior of different observables for the ground state of one-dimensional quenched disordered quantum Heisenberg (or XYZ)

models or quantum Heisenberg spin glass models. Specifically, we consider three paradigmatic classes of disordered Heisenberg spin glass Hamiltonians: the quenched disorder is in (a) the “planar” couplings, (b) the “azimuthal” couplings, and in (c) both the planar and azimuthal couplings. Although entanglement, especially multiparty entanglement, is known to be fragile, we find that both bipartite and multipartite entanglement can be enhanced by the introduction of all the disorder combinations mentioned. More important, and rather engrossing, is the uncovering of parameter ranges where the individual insertions of planar and azimuthal quenched disorder couplings do not result in disorder-induced enhancement of a multiparty entanglement measure, while the same appears in the simultaneous presence of the disorders. We term the phenomenon as constructive interference of the disordered couplings and the coupling parameter ranges as the Venus regions. Importantly, such constructive interference is not observed in single- as well as two-site physical quantities like magnetization, classical correlators, and bipartite entanglement. Moreover, changing the Hamiltonian, for example, to the XY model also wipes out the phenomena. Unlike the quantum XY disordered chain, for which the ground state can be handled by using the Jordan-Wigner transformation, the XYZ model, especially in the case of random couplings has to be addressed either by approximate methods or via numerical techniques. To study the different quenched physical quantities, we perform exact diagonalization for small systems and adapt density matrix renormalization group (DMRG) techniques [25] for larger systems, in order to obtain the zero temperature state. Multiparty entanglement is known to be an essential ingredient in several quantum information protocols. The results obtained have therefore the potential for important applications in actual realization of such protocols.

The counter intuitive nature of constructive interference for a physical quantity leads us to believe that it can have implications in fundamental and applicational regimes. Moreover, multiparty quantum informa-

tion processing tasks typically have origins in the bipartite domain. Instances where the converse occurs are few and far between, and indicates important diversions from the usual track (see e.g. [2, 26–28]). The fact that constructive interference is observed only for multipartite entanglement in the presence of impurities is also in the spirit of these latter instances.

The paper is organized as follows. In Sec. II, we introduce the quantum Heisenberg spin glass Hamiltonians of spin-1/2 particles and discuss the notion of quenched averaging. In Sec. III, we compare the physical quantities of disordered systems with those of ordered systems. We introduce the concept of enhancement score for a physical quantity and calculate it for single-site, bipartite and multipartite observables. Several cases of disorder-induced enhancement for different physical quantities are reported. The phenomenon of constructive interference is discussed in Sec. IV. Finally, we conclude in Sec. V.

II. THE ORDERED AND DISORDERED QUANTUM HEISENBERG MODELS

In this section, we first discuss the quenched averaging of a physical quantity and then we introduce the Hamiltonians that we investigate.

A. Quenched averaging

In the disordered models, that we consider here, the physical parameters of the system are “quenched”, i.e., the time scales in which the dynamics of the system takes place is much shorter in comparison to the time in which the disordered system parameters equilibrate. It implies that during the time-evolution of the system, a particular realization of the random disorder parameters remains frozen. The physically relevant values of the system observables (physical quantities) are, therefore, their quenched averaged values, where we first compute the value of the physical quantity of interest for a given disorder configuration of the system and subsequently perform the averaging over probability distribution of the disorder.

B. The Heisenberg quantum spin glasses

We now introduce the four different Heisenberg Hamiltonians which will be studied in this paper.

Case 0: The one-dimensional disordered quantum Heisenberg (or *XYZ*) model with nearest-neighbor interactions in an external magnetic field is described by

the Hamiltonian

$$H_{\langle J, \delta \rangle} = \kappa \left[\sum_{\langle i, j \rangle} \frac{J_{ij}}{4} [(1 + \gamma)\sigma_i^x \sigma_j^x + (1 - \gamma)\sigma_i^y \sigma_j^y] + \sum_{\langle i, j \rangle} \frac{\delta_{ij}}{4} \sigma_i^z \sigma_j^z - \frac{h}{2} \sum_i \sigma_i^z \right]. \quad (1)$$

Here, $J_{ij}(1 - \gamma)$ and $J_{ij}(1 + \gamma)$ are proportional to the *xx* and *yy* interactions, while δ_{ij} is that to the *zz* one. γ measures the anisotropy between the first two interactions, and is dimensionless. J_{ij} , δ_{ij} , and h are also dimensionless. κ is a constant, and has the units of energy. J_{ij} are independently and identically distributed (i.i.d.) Gaussian random variables with mean $\langle J \rangle$ and unit standard deviation. Similarly, δ_{ij} are i.i.d. Gaussian random variables with mean $\langle \delta \rangle$ and unit standard deviation. We set $\langle \lambda \rangle = \langle J \rangle / h$ and $\langle \mu \rangle = \langle \delta \rangle / h$, which are therefore again dimensionless. σ_i^k ($k = x, y, z$) are the Pauli spin matrices at the i^{th} site and $\langle i, j \rangle$ indicates that the corresponding summation is over nearest-neighbor spins. The applied field, h , is kept ordered throughout the paper.

Case 1: Quantum Heisenberg model. In this case, the Hamiltonian, which we denote by H , has site-independent couplings, i.e., $J_{ij} = J$ and $\delta_{ij} = \delta$. Since we will be in need of multisite state characteristics, the Bethe ansatz [29] is difficult to apply in an efficient way, especially in the disordered cases considered. We denote J/h and δ/h as λ and μ respectively.

Case 2: Quantum Heisenberg “planar” spin glass. The Hamiltonian in this case is given by

$$H_{\langle J \rangle} = \kappa \left[\sum_{\langle i, j \rangle} \frac{J_{ij}}{4} [(1 + \gamma)\sigma_i^x \sigma_j^x + (1 - \gamma)\sigma_i^y \sigma_j^y] + \sum_{\langle i, j \rangle} \frac{\delta}{4} \sigma_i^z \sigma_j^z - \frac{h}{2} \sum_i \sigma_i^z \right], \quad (2)$$

where the couplings δ_{ij} are considered to be site-independent, and fixed at δ .

Case 3: Quantum Heisenberg “azimuthal” spin glass. The system in this case is governed by the Hamiltonian, $H_{\langle \delta \rangle}$, in which $J_{ij} = J$, while the couplings, δ_{ij} , are i.i.d. Gaussian random variables with mean $\langle \delta \rangle$ and unit standard deviation.

III. ENHANCEMENT SCORE FOR THE QUENCHED DISORDERED SYSTEMS

Intuitively, disorder or defects in a system are supposed to have adverse effects on physical properties like magnetization, classical correlations, quantum correlation, etc. While this is true in many cases [30], there are also a significant number of physical systems, both classical and quantum, where certain physical properties get enhanced

in the presence of disorder, as compared to the corresponding clean systems [18, 19]. In this section, we first introduce a quantity called the “enhancement score” in order to quantify such disorder-induced advantage for a given quantity and then we study its behavior for different observables in Heisenberg spin glass systems.

A. Enhancement score and physical quantities

In a disordered system, if a quenched averaged physical quantity, \mathcal{Q}_{av} , associated with a state of the system is larger than the same quantity, \mathcal{Q} , of the corresponding ordered system in the analogous state, then the value of the physical quantity is said to exhibit a disorder-induced enhancement. To characterize such advantage, we introduce the enhancement score, $\Delta^{\mathcal{Q}}$, of a physical quantity \mathcal{Q} , which is defined as

$$\Delta_{a,b,\dots}^{\mathcal{Q}} = |\mathcal{Q}_{av}(\langle a \rangle, \langle b \rangle, \dots)| - |\mathcal{Q}(\langle a \rangle, \langle b \rangle, \dots)|. \quad (3)$$

Here, $\mathcal{Q}_{av}(\langle a \rangle, \langle b \rangle, \dots)$ is the quenched averaged value of a physical quantity, \mathcal{Q} , of the system where the averaging is performed over the system parameters, a, b, \dots , which follow Gaussian distributions with mean $\langle a \rangle, \langle b \rangle, \dots$ and standard deviations $\sigma_a, \sigma_b, \dots$ respectively. The definition can of course be generalized to the case of other probability distributions. $\mathcal{Q}(\langle a \rangle, \langle b \rangle, \dots)$ is the corresponding physical quantity for the ordered case of the same system, where the values of the system parameters a, b, \dots are kept constant (i.e., they are not disordered) at $\langle a \rangle, \langle b \rangle, \dots$ respectively. Both \mathcal{Q}_{av} and \mathcal{Q} will also usually depend on other systems parameters (that are not disordered) which are kept the same for both the systems (disordered and ordered) and which are kept silent in the notation. A positive enhancement score for a physical quantity, \mathcal{Q} , in a certain range of the system parameters will imply that “disorder-induced enhancement” or “order from disorder” is attained for \mathcal{Q} in that region of the parameter space. Where as a negative value of the same will indicate that \mathcal{Q} gets degraded.

In this paper, the physical quantities that we study are single-site observables like magnetization, two-site observables like classical correlators, and bipartite as well as multipartite quantum correlation measures. For the Heisenberg Hamiltonian, that we consider here, in both ordered as well as disordered cases, the x and y components of the magnetization of the ground state vanish, while the z component of the magnetization, $M_z^i = \text{Tr}(\sigma_i^z \rho_i^A)$, of the single-site reduced density matrix (ρ_i^A) at the i^{th} site of the ground state is in general non-vanishing. In the disordered case, one has to further perform a quenched averaging over the relevant variables to obtain the physically meaningful quenched averaged magnetization. The classical correlators between the i^{th} and j^{th} sites are defined as $T_{\alpha\beta}^{ij} = \text{Tr}(\sigma_i^\alpha \otimes \sigma_j^\beta \rho_{ij}^{AB})$ with $\alpha, \beta = x, y, z$ and ρ_{ij}^{AB} being the bipartite density matrix obtained from the ground state. It can be shown that

the off-diagonal correlators of the ground state vanish in both ordered and disordered cases [31].

Let us now define a measure to quantify nearest-neighbor bipartite entanglement in the ground state of these models. In case of bipartite entanglement, we first find the N -party ground state of a given Hamiltonian, and then we trace out all the $(N - 2)$ parties except two nearest-neighbor sites and subsequently consider the entanglement of that two-party state. In this work, we use the concurrence [32] as the bipartite entanglement measure. The concurrence, C_{AB} , of the nearest-neighbor bipartite state, ρ^{AB} , is defined as

$$C_{AB} = \max\{0, \lambda_1 - \lambda_2 - \lambda_3 - \lambda_4\}, \quad (4)$$

where λ_i ($i = 1, 2, 3, 4$) are the square roots of the eigenvalues of the matrix $\rho^{AB} \widetilde{\rho^{AB}}$, in decreasing order, and $\widetilde{\rho^{AB}} = (\sigma_A^y \otimes \sigma_B^y) \rho^{AB*} (\sigma_A^y \otimes \sigma_B^y)$, where complex conjugation is with respect to the computational basis.

As a measure of genuine multipartite entanglement measure, we will employ the generalized geometric measure (GGM) [33] (cf. [34]). In case of quantum systems composed of more than two subsystems, the quantification of entanglement is much more involved in comparison to the bipartite case. This is because in a multipartite scenario, there are qualitatively different kinds of entangled states like bi-separable, tri-separable, etc., and there are also genuine multipartite entangled states. For pure multiparty states, genuine multiparty entangled states are defined as those which are not product across any bi-partition. In order to quantify genuine multiparty entanglement, we use the GGM which is based on the distance between the N -party multipartite pure state, and an N -party pure state which is not genuinely multiparty entangled. More specifically, the GGM for an N -party pure quantum state, $|\psi_N\rangle$, is given by

$$\mathcal{E}(|\psi_N\rangle) = 1 - \max |\langle \phi_N | \psi_N \rangle|^2, \quad (5)$$

where the maximization is taken over all N -party pure quantum states, $|\phi_N\rangle$, that are not genuinely multiparty entangled. It is possible to evaluate the maximization analytically for an arbitrary state $|\psi_N\rangle$ and is given by

$$\mathcal{E}(\psi_N) = 1 - \max\{\eta_{\mathcal{A}:\mathcal{B}}^2 | \mathcal{A} \cup \mathcal{B} = \{1, \dots, N\}, \mathcal{A} \cap \mathcal{B} = \emptyset\}, \quad (6)$$

where $\eta_{\mathcal{A}:\mathcal{B}}$ is the maximal Schmidt coefficient of $|\psi_N\rangle$ in the bipartite split $\mathcal{A} : \mathcal{B}$.

B. Enhancement score for the Heisenberg quantum spin glasses

In this subsection, we investigate the behavior of different measurable quantities in all the three disordered models, introduced in Sec. II B. We compute the ground state in each of these models and investigate the behavior of the enhancement score, $\Delta_\xi^{\mathcal{Q}}$, corresponding to physical

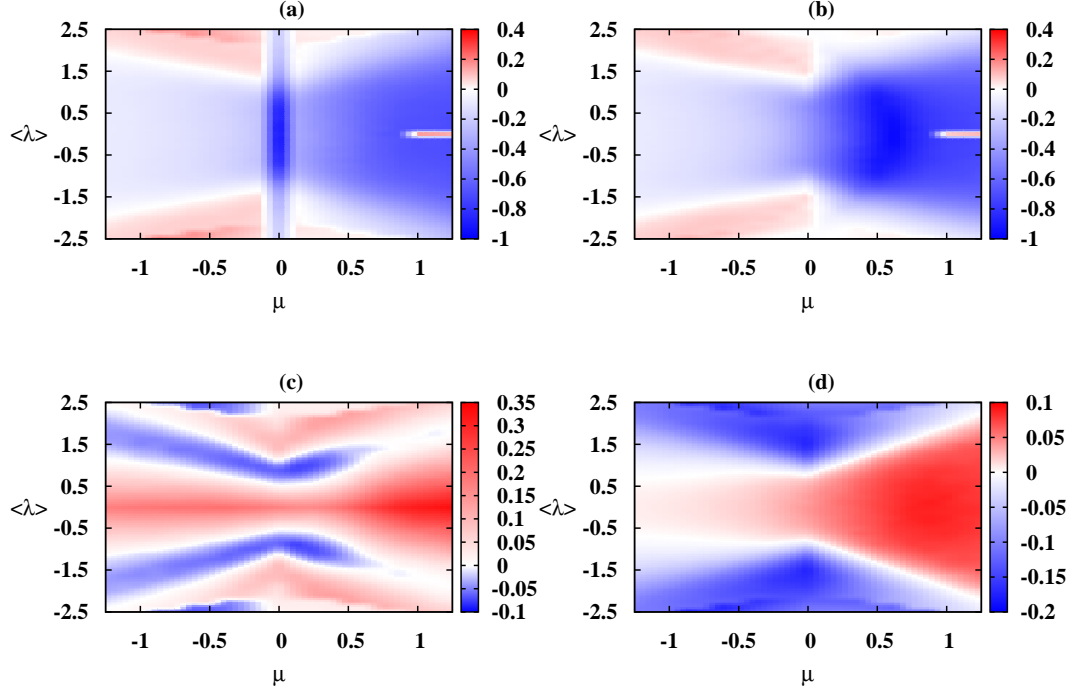


FIG. 1. (Color.) Order from disorder in the planar spin glass. The enhancement scores (Δ_λ^Q) for different physical quantities are plotted in the different panels. In all cases, the disordered Hamiltonian is $H_{(J)}$, while the ordered one is H . For the plots, we consider a system of 6 spins. And, we choose $\gamma = 0.7$ and $h = 0.8$. The planar spin glass Hamiltonian consists of 6 i.i.d Gaussian random variables, J_{ij} , which are each of mean $\langle J \rangle$ and standard deviation unity. The quantities that are plotted here are the enhancement scores for (a) magnetization ($\Delta_\lambda^{M_z}$), (b) the zz -classical correlator ($\Delta_\lambda^{T_{zz}}$) (c) bipartite quantum correlation as quantified by concurrence (Δ_λ^C), and (d) genuine multipartite quantum correlation measure quantified by GGM (Δ_λ^E). In these panels, the quantities along ordinates are $\langle \lambda \rangle$, while the abscissae represent the μ . Quenched average of the observable is performed over 5×10^3 random realizations. The regions represented in red are the ones for which Δ^Q is positive indicating that the corresponding physical quantity Q attains a higher value with the introduction of disorder in these regions. The areas represented in blue are the ones for which Δ^Q is negative and they point to parameter regions where the Q is higher in the corresponding clean system. In the white regions, Q remains unaltered by the introduction of disorder in the system. All the parameters plotted here are dimensionless.

quantities like transverse magnetization, classical correlations, concurrence, and generalized geometric measure. Here, ξ denotes the aggregate of system parameters that are quenched disordered. There is a wide range of the anisotropy parameter, γ , and magnetic field strength, h , of these models for which order from disorder phenomena of several quantities of the ground state are observed. For the purpose of depiction of the effects, throughout this paper, we choose $\gamma = 0.7$ and $h = 0.8$. However, it is worth mentioning that the qualitative behavior of all the observables in the disordered as well as in the ordered cases remain unchanged with the variation of γ and h . Quantitatively, the values of enhancement score of the quantities increase or decrease with the change of the system parameters, like anisotropy, coupling strengths, and magnetic field. Interestingly, we find that in all these models, there are large surfaces in the parameter space in which the magnetization and classical correlators behave in a complementary way to bipartite and multipartite entanglement, i.e., when $\Delta_\xi^{M_z}$, $\Delta_\xi^{T_{zz}}$ are positive, Δ_ξ^C , Δ_ξ^E

are negative, and vice versa.

In the following cases of the disordered systems, quenched averaging is performed over 5×10^3 realizations. For fixed values of $\langle \lambda \rangle$, $\langle \delta \rangle$, and h , we have performed the numerical simulations for higher number of realizations and have found that the corresponding quenched physical quantities have already converged for 5×10^3 realizations or before.

1. Order from disorder in planar spin glass

We investigate here the behavior of enhancement scores of different physical quantities for the case when the disorder is introduced in the planar coupling, i.e., in the xx - and yy -couplings. The Hamiltonian for such a system is given in Eq. (2). In Fig. 1, we show the behavior of the enhancement scores of magnetization, zz -correlator, concurrence, and GGM, with the variation of $\langle \lambda \rangle$ and μ . In all the cases considered, we have observed

disorder-induced enhancement also for T_{xx} and T_{yy} . We do not exhibit them in the figures given.

The investigation shows that for all observables, there exist regions in which the enhancement score is vanishing. These appear as white regions in the panels in Figs. 1, 2, and 3. Also, for large mean values of the disordered interactions, where the simultaneous presence of ferro- and anti-ferromagnetic couplings due to the disorder is absent, the enhancement scores vanish. These features are true for all types of disorder considered here.

In all the observables considered, viz. magnetization, classical correlators, and bipartite as well as multipartite entanglement, for a given μ , there typically appears oscillations in the surface of the enhancement score as we scan the $\langle\lambda\rangle$ axis and occasionally such oscillations have a positive enhancement score in their crests and negative one in their troughs. The parameter regions, which have a positive enhancement for a certain physical quantity, indicates an order from disorder phenomenon for that quantity. See Fig. 1 for a depiction.

2. Order from disorder in azimuthal spin glass

We now move on to study the behavior of the enhancement scores of physical quantities, when the disorder is introduced in the “azimuthal” coupling, for which the Hamiltonian is introduced as Case 3 in Sec. II B. In Fig. 2, we plot the physical quantities, m_z , T_{zz} , C , and \mathcal{E} , with respect to the planar coupling constant, λ , and the mean azimuthal coupling constant, $\langle\mu\rangle$. We have chosen the anisotropy constant as 0.7 and the external applied magnetic field as 0.8, as before.

As seen in the panels of Fig. 2, there are again order from disorder phenomena for all the observables considered. The behavior of the enhancement scores for magnetization and classical correlators are quite similar to those in the proceeding case. For concurrence and GGM, there are some differences. In particular, the $\lambda = 0$ line has $\Delta_\mu^C \approx 0$ in this case, while in the preceding case, the $\langle\lambda\rangle = 0$ line had $\Delta_\lambda^C > 0$.

3. The case of disorder in both planar and azimuthal couplings

When both planar and azimuthal couplings are disordered (see Eq. (1)), one may expect that the effects of disorder may suppress the physical quantities in a stronger way, and result in a complete absence of phenomena akin to “order from disorder”. However, we find that this is not the case. All the observables that we consider again exhibit regions in which disorder-induced order can be seen (as shown in Fig. 3).

IV. CONSTRUCTIVE INTERFERENCE BETWEEN PLANAR AND AZIMUTHAL COUPLINGS IN GGM

The Hamiltonian that we study involve planar and azimuthal interaction strengths, which may both be Gaussian distributed quenched disordered variables. We have already seen that irrespective of whether they are individually or jointly present, a spectrum of measurable quantities show order from disorder, instead of getting diminished in the presence of defects. At this juncture, we ask a more radical question: *Does there exist any observable which gets enhanced in the joint presence of the disorders while it deteriorates when the randomness is applied individually in either of the couplings, in the Heisenberg spin glass models?* Mathematically, we are looking for the following conditions to be satisfied simultaneously by an observable \mathcal{Q} :

$$\Delta_{\lambda,\mu}^{\mathcal{Q}} = |\mathcal{Q}_{av}(\langle\lambda\rangle, \langle\mu\rangle)| - |\mathcal{Q}(\langle\lambda\rangle, \langle\mu\rangle)| > 0, \quad (7a)$$

$$\Delta_\lambda^{\mathcal{Q}} = |\mathcal{Q}_{av}(\langle\lambda\rangle)| - |\mathcal{Q}(\langle\lambda\rangle)| < 0, \quad (7b)$$

$$\Delta_\mu^{\mathcal{Q}} = |\mathcal{Q}_{av}(\langle\mu\rangle)| - |\mathcal{Q}(\langle\mu\rangle)| < 0. \quad (7c)$$

Here, $\mu = \langle\mu\rangle$ in Eq. (7b) and $\mathcal{Q}_{av}(\langle\lambda\rangle)$ corresponds to the planar spin glass. Similarly, $\lambda = \langle\lambda\rangle$ in Eq. (7c) and $\mathcal{Q}_{av}(\langle\mu\rangle)$ corresponds to the azimuthal spin glass. Any observable satisfying the above set of equations would imply that the competing random interactions can interfere constructively for the quantity \mathcal{Q} . We refer to this phenomenon as the “constructive interference of \mathcal{Q} ”.

We have extensively investigated the above equations for various finite number of spins in the Heisenberg Hamiltonian ranging from $N = 5$ to $N = 20$, and scanned over significant ranges of the system parameters. While smaller system sizes are handled by exact diagonalization, the relatively larger ones are investigated by employing the density matrix renormalization group techniques. The investigations help us to identify certain parameter ranges, where the system exhibits the phenomenon of the constructive interference in the genuine multipartite quantum correlation measure, GGM. Interestingly, no other observable, considered here, shows such a behavior.

A. Constructive interference in systems realizable with current technology

Let us first discuss the results corresponding to the Heisenberg spin glass models, consisting of a comparatively small number of spins. The behavior of quantum correlations, in this case can be examined in experimentally realizable systems like ion traps, photons, etc [5–8], and hence the results obtained in this subsection can be verified and observed in the laboratories. All the results presented in this subsection are obtained by performing exact diagonalization of the Hamiltonians. Fig. 4 shows

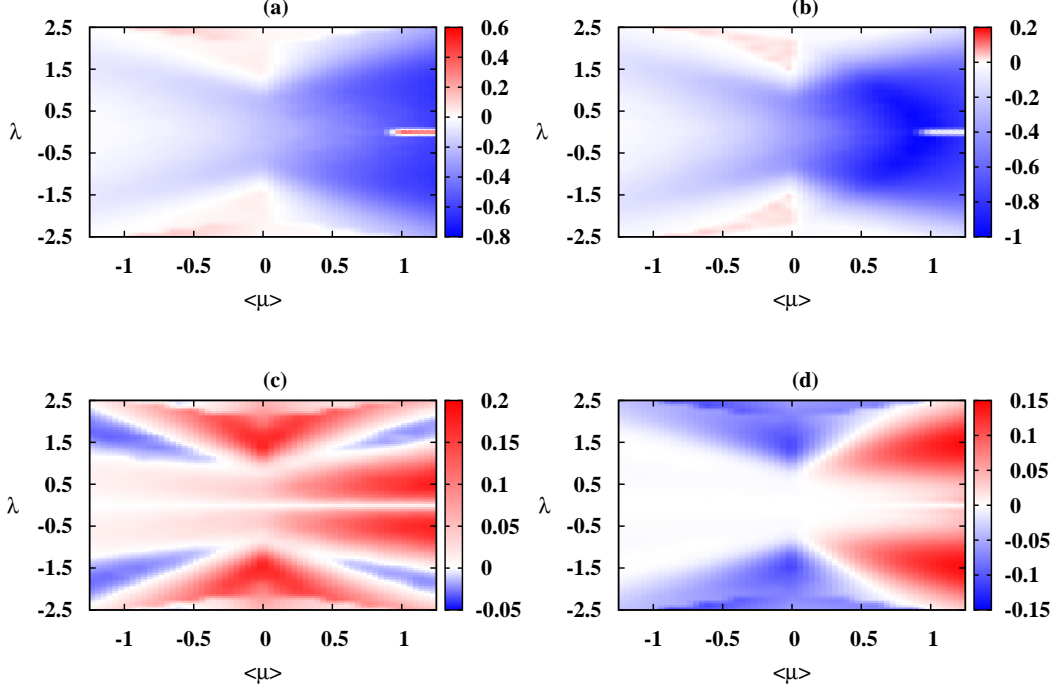


FIG. 2. (Color.) Order from disorder in azimuthal spin glass. The plots in the different panels are for (a) Δ_μ^{Mz} , (b) Δ_μ^{Tzz} , (c) Δ_μ^C , and (d) Δ_μ^ε . The disordered Hamiltonian for the enhancement scores is $H_{\langle \delta \rangle}$, whose 6 i.i.d. Gaussian random variables, δ_{ij} , have mean $\langle \delta \rangle$ and unit standard deviation. In each of these panels, the ordinate is λ and the abscissa is $\langle \mu \rangle$. All other considerations are the same as in Fig. 1.

the enhancement scores for the GGM for different system sizes, and for different blending of disordered couplings. The anisotropy and external magnetic field strength are again chosen as 0.7 and 0.8 respectively. The coupling strength, δ , in the azimuthal direction, is -0.9 for the case when it is ordered, while in the cases when the azimuthal couplings, δ_{ij} , are disordered, they are chosen with mean -0.9 and unit standard deviation.

Whenever any of the curves, in the panels of Fig. 4, is positive, the corresponding disordered system has higher value of GGM as compared to that of the ordered system. It is clear from Fig. 4 that $\Delta_\lambda^\varepsilon$, Δ_μ^ε , as well as $\Delta_{\lambda,\mu}^\varepsilon$ show order from disorder, although in different parameters ranges. There are several other parameter ranges than those exhibited in the panels of Fig. 4 where such phenomenon occurs. The choice of the parameters and parameter ranges in Fig. 4 are for the following specific purpose. Near the two values of α ($= \langle \lambda \rangle$, here), where the curves of $\Delta_{\lambda,\mu}^\varepsilon$ crosses the horizontal axes, one obtains regions where order from disorder for GGM is exhibited with the introduction of both planar and azimuthal disorders, while the same is absent with the inclusion of just any one of these disorders. We call these as “Venus regions”. For example, for $N = 6$ (see Fig. 4(b)), the two distinct ranges of α (which represents either $\langle \lambda \rangle$ or λ), in which the constructive interference can be observed are $[-0.78, -0.67]$ and $[0.68, 0.78]$. In

these regions, the enhancement score, $\Delta_{\lambda,\mu}^\varepsilon$ (red circles connected by dashed line), is positive while the other two enhancement scores, viz., the $\Delta_\lambda^\varepsilon$ (blue squares connected by dotted line) and Δ_μ^ε (green triangles connected by dot-dashed line), remain negative. Note that with increasing number of particles, the Venus regions, i.e., the windows of α demonstrating constructive interference moves towards $\alpha = 0$. Interestingly, no such phenomenon is found in other quantities considered in this paper, viz., magnetization, two-point correlators, and bipartite entanglement (see Fig. 5). It is worth mentioning here that the Venus regions do not surface without an external magnetic field. In fact, depending on N , there exists a critical magnetic field strength, h_c , only beyond which the constructive interference can be observed. Below h_c , the $\Delta_\lambda^\varepsilon$ lies above the $\Delta_{\lambda,\mu}^\varepsilon$ and the Δ_μ^ε . As the external magnetic field is increased beyond h_c , the curve corresponding to the $\Delta_{\lambda,\mu}^\varepsilon$ goes above that of $\Delta_\lambda^\varepsilon$ and Δ_μ^ε , resulting in the emerging of the Venus regions. We find that the h_c is approximately 0.6 for $N = 6$.

B. Approximate GGM and sustenance of Venus regions in larger systems

It is natural to ask if the results presented in the previous subsection also holds for the disordered Heisenberg

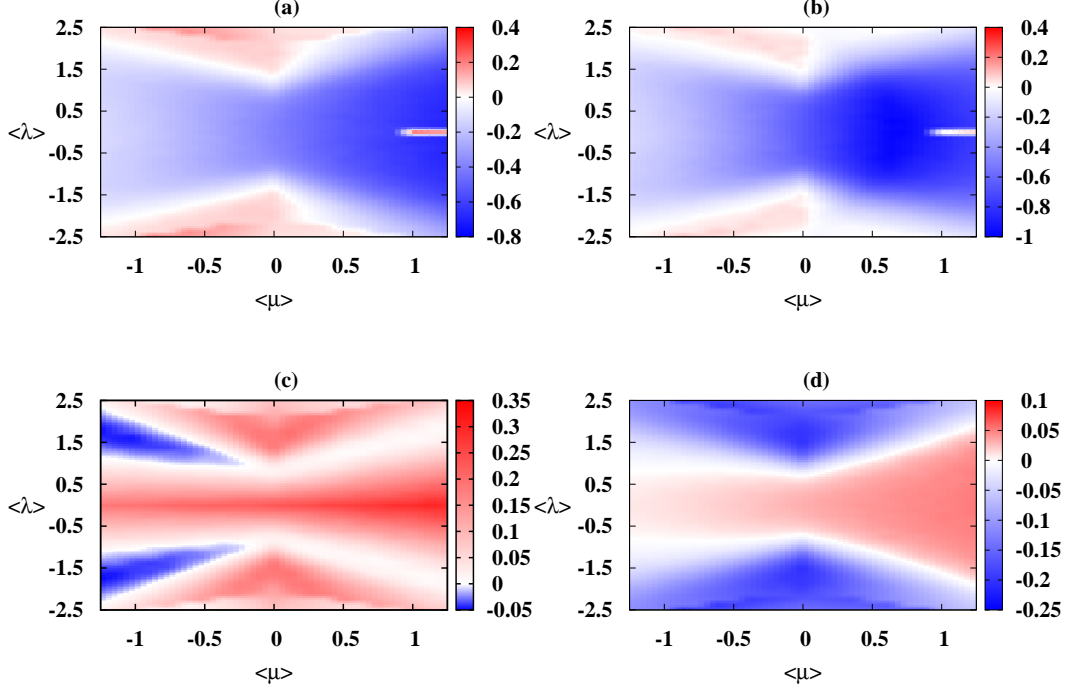


FIG. 3. (Color.) Order from disorder when both planar and azimuthal couplings are quenched disordered. The plots in the different panels are for (a) $\Delta_{\lambda,\mu}^{Mz}$, (b) $\Delta_{\lambda,\mu}^{Tzz}$, (c) $\Delta_{\lambda,\mu}^C$, and (d) $\Delta_{\lambda,\mu}^E$. The disordered Hamiltonian in this case is $H_{\langle J,\delta \rangle}$. The J_{ij} (δ_{ij}) are i.i.d. Gaussian random variables with mean $\langle J \rangle$ ($\langle \delta \rangle$) and unit standard deviation. In the panels, the ordinates represent $\langle \lambda \rangle$ while the abscissae represent $\langle \mu \rangle$. All other considerations are as in Fig. 1.

systems with larger number of spins. However, exact computation of the quenched averaged GGM, in systems with large number of parties, is hindered, due to the following three key reasons: (i) An exponential growth of the Hilbert space with increasing number of parties essentially prohibits one from performing exact diagonalization of the Hamiltonian. (ii) For obtaining the desired accuracy, as one tries to obtain convergence in the quenched averaging of physical quantities, it typically requires a large number (approximately 5×10^3 to 8×10^3) of random realizations, unless the quantities are self-averaging, which is not the case for all genuine multipartite observables. (iii) Determination of multipartite entanglement, as quantified by the GGM, requires all possible bipartite splits, and the number of bipartitions in an N -party system is $\sum_{r=1}^{N/2} \binom{N}{r}$, which increases substantially with increasing N . For example, the number of bipartitions required to evaluate the GGM for the $N = 8$ system is 162, whereas it grows to over half a million for the system involving just 20 parties.

The difficulty in computing GGM can partly be curbed by choosing selective bipartitions instead of considering all possible bipartitions. We therefore introduce $\mathcal{E}^{(2)}$ as a measure of multipartite entanglement, defined as

$$\mathcal{E}^{(2)} = 1 - \max \left\{ \{ \eta_i^2 \}, \{ \eta_{i,i+1}^2 \} \mid i=1, \dots, N \right\}, \quad (8)$$

where η_i and $\eta_{i,i+1}$ are the maximum Schmidt coeffi-

cients of the single- and nearest-neighbor two-body reduced density matrices respectively. We call it the “approximate GGM”. Although $\mathcal{E}^{(2)}$ may not be a *genuine* multipartite entanglement measure, it does quantify multipartite entanglement and it is certainly an entanglement monotone.

In order to perform numerical simulations with larger number of spins, we adopt the finite size density matrix renormalization group method [25] with the open boundary condition in the system, which is an iterative numerical approach for obtaining highly accurate low energy physics of quantum many-body systems. In the DMRG approach, starting from a portion of the system, known as system block, the system size is enlarged step by step until the desired system size is reached. The value of physical quantities for the disordered spin chain can be achieved by performing several sweeps of the finite system DMRG [25]. We choose to work with open boundary conditions as it is well known that the accuracy drops significantly for closed boundary conditions. For N -site systems, the bipartite classical and quantum correlations are calculated for the $(N/2, N/2 + 1)$ pairs, so that boundary effect are minimized.

For the Heisenberg spin models with and without disorder, we evaluate the approximate GGM and plot the enhancement scores in Fig. 6. Here we consider the spin systems with sizes $N = 8$ (Fig. 6(a)), $N = 12$ (Fig. 6(b)),

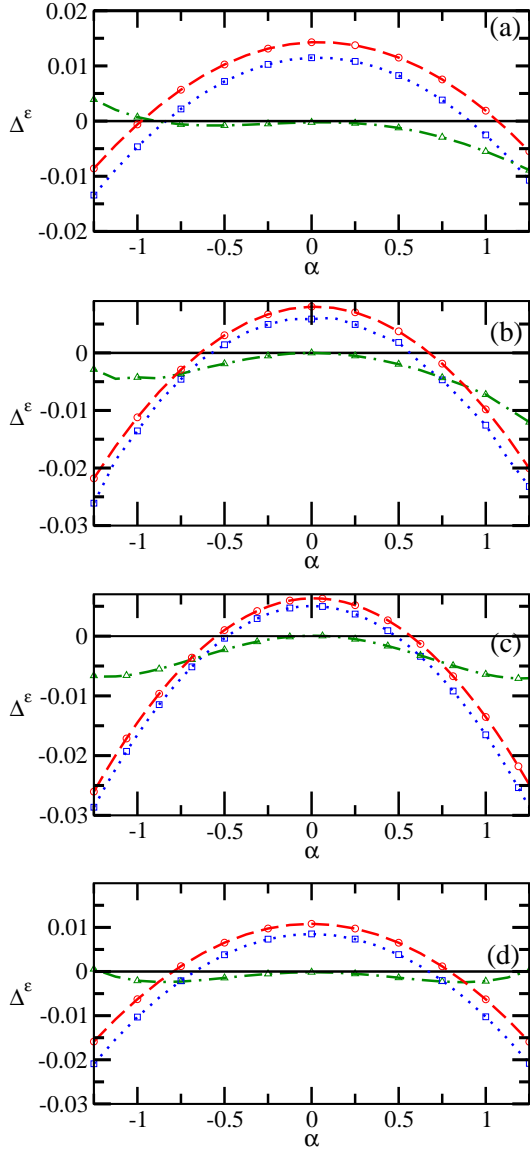


FIG. 4. (Color online.) Constructive interference. The panels exhibit plots with the enhancement score of GGM, denoted as Δ^ε , as the ordinate, and the system parameter, α , as the abscissa for Heisenberg spin glasses with (a) $N = 5$, (b) $N = 6$, (c) $N = 7$, and (d) $N = 8$, where N is the number of quantum spin-1/2 particles in the system. In all these plots, red circles connected with dashed lines represent the cases when disorder is present in both the couplings (planar as well as azimuthal), and for these cases, α represents $\langle \lambda \rangle$ and Δ^ε represents $\Delta_{\lambda,\mu}^\varepsilon$. We choose $\langle \delta \rangle = -0.9$. The blue squares connected with dotted lines are for the cases when disorder is present only in the planar coupling. In these cases, α represents $\langle \lambda \rangle$, Δ^ε represents $\Delta_\lambda^\varepsilon$, and δ is fixed at -0.9 . The green triangles connected with dash-dotted lines represent the cases when disorder is present only in the azimuthal coupling. In these cases, α represents λ , Δ^ε represents Δ_μ^ε , and $\langle \delta \rangle = -0.9$. The black solid lines, parallel to the horizontal axes are drawn to separate the positive and negative regions of the enhancement score of GGM. For all the plots, we have chosen $\gamma = 0.7$ and $h = 0.8$. All quantities plotted here are dimensionless.

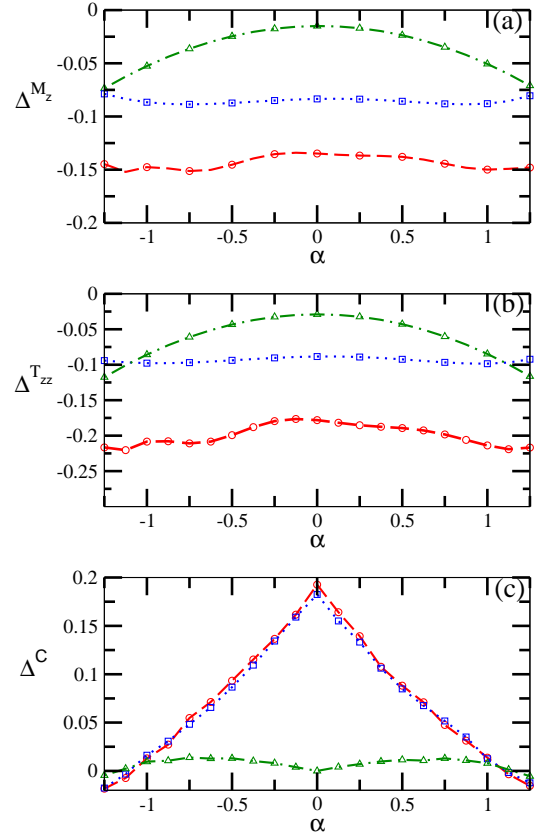


FIG. 5. (Color online.) The enhancement scores for (a) magnetization, M_z , (b) T_{zz} -correlator, and (c) concurrence, C , against α for systems with $N = 6$. All other descriptions are the same as given in Fig. 4.

$N = 16$ (Fig. 6(c)), and $N = 20$ (Fig. 6(d)). The symbols are kept consistent with Fig. 4. It can clearly be noticed that the $\Delta^{\varepsilon^{(2)}}$ again identify two distinct ranges of the parameter α (on the negative and positive sides of α), where the Venus regions materialize. We also find that the conclusions drawn from the $\mathcal{E}^{(2)}$ are consistent with the physics discussed by studying the system with smaller sizes. For example, the windows of α exhibiting constructive interference shifts towards $\alpha = 0$ with increasing number of spins. We find that even for $N = 20$, there is a non-zero region where constructive interference occurs. It is to be noted the shrinking observed, of the Venus regions, could be due to the modification of the multiparty party entanglement measure, since we have already observed that no two-party or single-site observables exhibit the constructive interference. It is plausible that in the presence of both the disorders, multipartite entanglement will exhibit a Venus region even in the thermodynamical limit. We additionally investigate the magnetization, two-point correlations in the zz direction and the concurrence in this regime. Fig. 7 shows their behavior for $N = 20$. We find no constructive interference phenomena in any of these quantities.

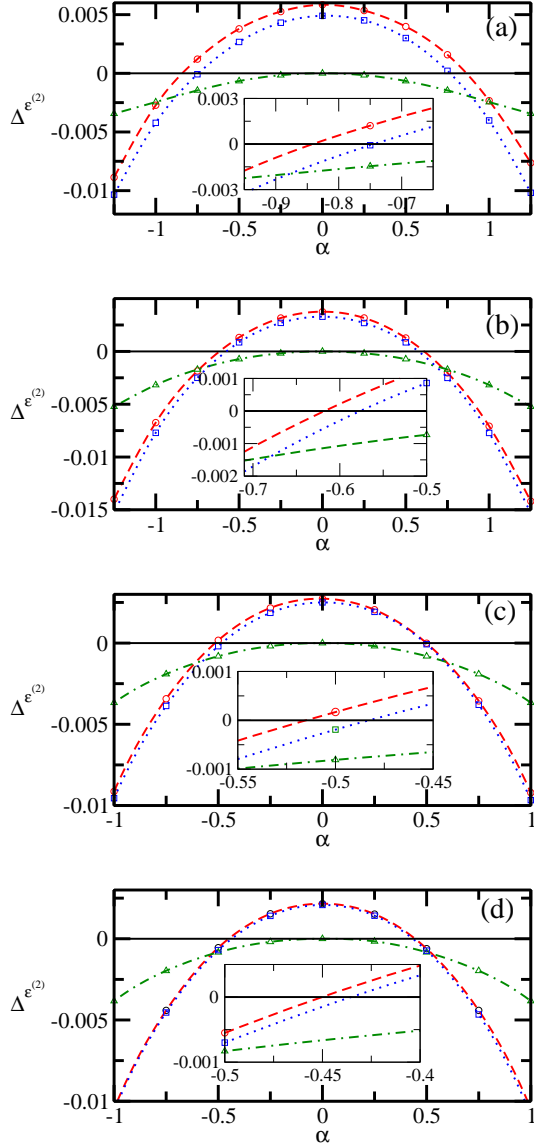


FIG. 6. (Color online.) DMRG data of the enhancement score $\Delta\epsilon^{(2)}$ as a function of α for (a) $N = 8$, (b) $N = 12$, (c) $N = 16$, and (d) $N = 20$. All other descriptions are the same as in Fig. 4. The insets show blow-ups of the regions with constructive interference.

V. CONCLUSION

In summary, we have studied the quantum Heisenberg spin system in one-dimension with random coupling interactions. We have examined the behavior of the magnetization, classical as well as the two-party quantum correlations, and multipartite entanglement for the ground states. The relevant results are presented for various system sizes ranging from five to twenty quantum spin-1/2 particles. While the small systems were dealt by exact numerical diagonalization, we adopt the density matrix renormalization technique to investigate comparatively

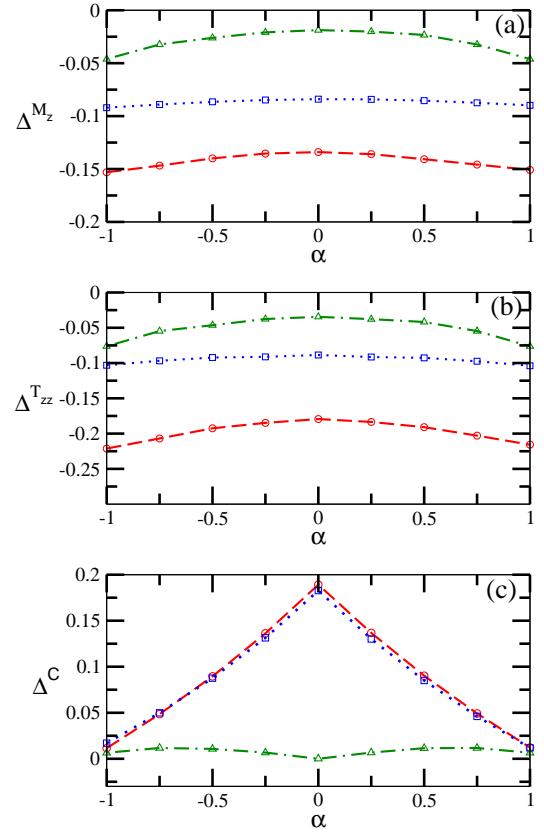


FIG. 7. (Color online.) The DMRG data of the enhancement scores for (a) magnetization, M_z (b) classical correlator, T_{zz} , and (c) concurrence for systems with $N = 20$. All other considerations are the same as given in Fig. 4. The magnetizations used here in panel (a) are for the site $N/2$.

larger spin systems. In the presence of impurities in the couplings, there exists different parameter regions for the different observables which show enhancement due to disorder – also known as the order from disorder phenomenon. The physical quantities like magnetization, classical correlators, bipartite and multipartite entanglement always find a range of parameters in which they increase with the introduction of disorder. Our studies uncover the phenomenon of constructive interference, where we observe that the parameters of the system can be tuned in such a way that disorder-induced order appears due to simultaneous presence of randomness in two different couplings, while it is absent when disorder is present individually in either of the couplings.

The constructive interference, which is caused due to the interplay between competing random coupling strengths in different directions, appears only in the multipartite entanglement, and is absent in bipartite as well as single-site physical quantities considered.

ACKNOWLEDGMENTS

We acknowledge the useful discussions with Luigi Amico during the meeting on Quantum Information Processing and Applications (QIPA-2013) held at the Harish-Chandra Research Institute (HRI), India. RP acknowledges support from the Department of Science and Tech-

nology, Government of India, in the form of an INSPIRE faculty scheme at HRI. We acknowledge computations performed at the cluster computing facility in HRI. This work has been developed by using the DMRG code released within the Powder with Power project (www.dmrp.it).

-
- [1] M. Żukowski, A. Zeilinger, M. A. Horne, and H. Weinfurter, *Acta Phys. Pol. A* **93**, 187 (1998); M. Hillery, V. Bužek, and A. Berthiaume, *Phys. Rev. A* **59**, 1829 (1999); A. Karlsson, M. Koashi, and N. Imoto, *ibid.* **59**, 162 (1999); R. Cleve, D. Gottesman, and H.-K. Lo, *Phys. Rev. Lett.* **83**, 648 (1999); D. Gottesman, *Phys. Rev. A* **61**, 042311 (2000); W. Tittel, H. Zbinden, and N. Gisin, *ibid.* **63**, 042301 (2001); S. K. Singh and R. Srikanth, *ibid.* **71**, 012328 (2005); Z.-j. Zhang, Y. Li, and Z.-x. Man, *ibid.* **71**, 044301 (2005); K. Chen and H.-K. Lo, *Quantum Inf. Comput.* **7**, 689 (2007); D. Markham and B. C. Sanders, *Phys. Rev. A* **78**, 042309 (2008); R. Demkowicz-Dobrzański, A. Sen(De), U. Sen, and M. Lewenstein, *ibid.* **80**, 012311 (2009); A. Marin and D. Markham, *ibid.* **88**, 042332 (2013).
 - [2] R. Raussendorf and H. J. Briegel, *Phys. Rev. Lett.* **86**, 5188 (2001); F. Meier, J. Levy, and D. Loss, *ibid.* **90**, 047901 (2003); R. Raussendorf, D. E. Browne, and H. J. Briegel, *Phys. Rev. A* **68**, 022312 (2003); M. A. Nielsen, *Phys. Rev. Lett.* **93**, 040503 (2004); P. Walther, K. J. Resch, T. Rudolph, E. Schenck, H. Weinfurter, V. Vedral, M. Aspelmeyer, and A. Zeilinger, *Nature* **434**, 169 (2005); M. A. Nielsen, *Rep. Math. Phys.* **57**, 147 (2006); H. J. Briegel, D. E. Browne, W. Dür, R. Raussendorf, and M. V. den Nest, *Nat. Phys.* **5**, 19 (2009).
 - [3] S. Bose, *Contemporary Physics* **48**, 13 (2007); G. M. Nikolopoulos and I. Jex, *Quantum State Transfer and Network Engineering* (Springer, Heidelberg, 2013).
 - [4] C. H. Bennett and S. J. Wiesner, *Phys. Rev. Lett.* **69**, 2881 (1992); K. Mattle, H. Weinfurter, P. G. Kwiat, and A. Zeilinger, *ibid.* **76**, 4656 (1996); D. Bruß, G. M. D'Ariano, M. Lewenstein, C. Macchiavello, A. Sen(De), and U. Sen, *ibid.* **93**, 210501 (2004).
 - [5] D. Leibfried, R. Blatt, C. Monroe, and D. Wineland, *Rev. Mod. Phys.* **75**, 281 (2003); H. Häffner, C. Roos, and R. Blatt, *Phys. Rep.* **469**, 155 (2008).
 - [6] T. E. Northup and R. Blatt, *Nat. Photonics* **8**, 356 (2014).
 - [7] I. Bloch, *J. Phys. B: At. Mol. Opt. Phys.* **38**, S629 (2005); P. Treutlein, T. Steinmetz, Y. Colombe, B. Lev, P. Hommelhoff, J. Reichel, M. Greiner, O. Mandel, A. Widera, T. Rom, I. Bloch, and T. W. Hänsch, *Fortschr. Phys.* **54**, 702 (2006).
 - [8] Y. Makhlin, G. Schön, and A. Shnirman, *Rev. Mod. Phys.* **73**, 357 (2001); D. Vion, A. Aassime, A. Cottet, P. Joyez, H. Pothier, C. Urbina, D. Esteve, and M. Devoret, *Science* **296**, 866 (2002); M. H. Devoret, A. Wallraff, and J. M. Martinis, *arXiv:cond-mat/0411174*; J. Q. You and F. Nori, *Phys. Today* **58**, 42 (2005); G. Wendin and V. Shumeiko, *Handbook of Theoretical and Computational Nanotechnology* (American Scientific Publishers, 2006), chap. Superconducting Quantum Circuits, Qubits and Computing; J. Clarke and F. Wilhelm, *Nature (London)* **453**, 1031 (2008).
 - [9] R. Horodecki, P. Horodecki, M. Horodecki, and K. Horodecki, *Rev. Mod. Phys.* **81**, 865 (2009).
 - [10] S. Sachdev, *Quantum Phase Transitions* (Cambridge University Press, Cambridge, 1999).
 - [11] M. Lewenstein, A. Sanpera, V. Ahufinger, B. Damski, A. Sen(De), and U. Sen, *Adv. Phys.* **56**, 243 (2007).
 - [12] L. Amico, R. Fazio, A. Osterloh, and V. Vedral, *Rev. Mod. Phys.* **80**, 517 (2008).
 - [13] F. Verstraete, J. I. Cirac, and V. Murg, *Adv. Phys.* **57**, 143 (2008); G. Vidal, *Phys. Rev. Lett.* **101**, 110501 (2008); A. J. Ferris and G. Vidal, *Phys. Rev. B* **85**, 165147 (2012), and references therein.
 - [14] W. G. Brown, L. F. Santos, D. J. Starling, and L. Viola, *Phys. Rev. E* **77**, 021106 (2008); G. Refael and J. E. Moore, *J. Phys. A: Math. Theor.* **42**, 504010 (2009).
 - [15] F. C. Nix and W. Shockley, *Rev. Mod. Phys.* **10**, 1 (1938); P. Dean, *ibid.* **44**, 127 (1972); R. J. Elliott, J. A. Krumhansl, and P. L. Leath, *ibid.* **46**, 465 (1974); A. S. Barker, Jr. and A. J. Sievers, *ibid.* **47**, S1 (1975); P. A. Lee and T. V. Ramakrishnan, *ibid.* **57**, 287 (1985); A. G. Aronov and Yu. V. Sharvin, *ibid.* **59**, 755 (1987); J. C. Dyre and T. B. Schröder, *ibid.* **72**, 873 (2000).
 - [16] F. Iglói and C. Monthus, *Phys. Rep.* **412**, 277 (2005).
 - [17] G. Misguich and C. Lhuillier, *Frustrated Spin Systems*, edited by H. T. Diep (World-Scientific, Singapore, 2005).
 - [18] A. Aharony, *Phys. Rev. B* **18**, 3328 (1978); J. Villain, R. Bidaux, J.-P. Carton, and R. Conte, *J. Physique* **41**, 1263 (1980); B. J. Minchau and R. A. Pelcovits, *Phys. Rev. B* **32**, 3081 (1985); C. L. Henley, *Phys. Rev. Lett.* **62**, 2056 (1989); A. Moreo, E. Dagotto, T. Jolicœur, and J. Riera, *Phys. Rev. B* **42**, 6283 (1990); D. E. Feldman, *J. Phys. A* **31**, L177 (1998); G. E. Volovik, *JETP Lett.* **84**, 455 (2006); D. A. Abanin, P. A. Lee, and L. S. Levitov, *Phys. Rev. Lett.* **98**, 156801 (2007); L. Adamska, M. B. Silva Neto, and C. Morais Smith, *Phys. Rev. B* **75**, 134507 (2007); A. Niederberger, T. Schulte, J. Wehr, M. Lewenstein, L. Sanchez-Palencia, and K. Sacha, *Phys. Rev. Lett.* **100**, 030403 (2008); A. Niederberger, J. Wehr, M. Lewenstein, and K. Sacha, *Europhys. Lett.* **86**, 26004 (2009); A. Niederberger, M. M. Rams, J. Dziarmaga, F. M. Cucchiatti, J. Wehr, and M. Lewenstein, *Phys. Rev. A* **82**, 013630 (2010); D. I. Tsomokos, T. J. Osborne, and C. Castelnovo, *Phys. Rev. B* **83**, 075124 (2011); M. S. Foster, H.-Y. Xie, and Y.-Z. Chou, *ibid.* **89**, 155140 (2014); P. Villa Martín, J. A. Bonachela, and M. A. Muñoz, *Phys. Rev. E* **89**, 012145 (2014), and references therein.
 - [19] L. F. Santos, G. Rigolin, and C. O. Escobar, *Phys. Rev. A* **69**, 042304 (2004); C. Mejía-Monasterio, G. Benenti, G. G. Carlo, and G. Casati, *ibid.* **71**, 062324 (2005); A. Lakshminarayan and V. Subrahmanyam, *ibid.* **71**, 062334

- (2005); R. López-Sandoval and M. E. Garcia, Phys. Rev. B **74**, 174204 (2006); J. Karthik, A. Sharma, and A. Lakshminarayan, Phys. Rev. A **75**, 022304 (2007); W. G. Brown, L. F. Santos, D. J. Sterling, and L. Viola, Phys. Rev. E **77**, 021106 (2008); F. Dukesz, M. Zilbergerts, and L. F. Santos, New J. Phys. **11**, 043026 (2009); J. Hide, W. Son, and V. Vedral, Phys. Rev. Lett. **102**, 100503 (2009); K. Fujii and K. Yamamoto, Phys. Rev. A **82**, 042109 (2010); R. Prabhu, S. Pradhan, A. Sen(De), and U. Sen, Phys. Rev. A **84**, 042334 (2011), and references therein.
- [20] K. Binder and A. P. Young, Rev. Mod. Phys. **58**, 801 (1986); D. Belitz, T. R. Kirkpatrick, and T. Vojta, *ibid.* **77**, 579 (2005); A. Das and B. K. Chakrabarti, *ibid.* **80**, 1061 (2008); H. Alloul, J. Bobroff, M. Gabay, and P. J. Hirschfeld, *ibid.* **81**, 45 (2009).
- [21] J. P. Á. Zúñiga and N. Laflorencie, Phys. Rev. Lett. **111**, 160403 (2013); Z. Yao, K. P. C. da Costa, M. Kiselev, and N. Prokofev, *ibid.* **112**, 225301 (2014), and references therein.
- [22] P. W. Anderson, Phys. Rev. **109**, 1492 (1958); E. Abrahams, P. W. Anderson, D. C. Licciardello, and T. V. Ramakrishnan, Phys. Rev. Lett. **42**, 673 (1979); P. A. Lee and T. V. Ramakrishnan, Rev. Mod. Phys. **57**, 287 (1985); B. Kramer and A. MacKinnon, Rep. Prog. Phys. **56**, 1469 (1993).
- [23] E. Dagotto, Rev. Mod. Phys. **66**, 763 (1994); P. A. Lee, N. Nagaosa, and X.-G. Wen, Rev. Mod. Phys. **78**, 17 (2006); X.-L. Qi and S.-C. Zhang, Rev. Mod. Phys. **83**, 1057 (2011), and references therein.
- [24] L. Fallani, J. E. Lye, V. Guarnera, C. Fort, and M. Inguscio, Phys. Rev. Lett. **98**, 130404 (2007); G. Roati, C. D'Errico, L. Fallani, M. Fattori, C. Fort, M. Zaccanti, G. Modugno, M. Modugno, and M. Inguscio, Nature **453**, 895 (2008); J. Billy, V. Josse, Z. Zuo, A. Bernard, B. Hambrecht, P. Lugan, D. Clément, L. Sanchez-Palencia, P. Bouyer, and A. Aspect, *ibid.* **453**, 891 (2008); R. Yu, L. Yin, N. S. Sullivan, J. S. Xia, C. Huan, A. Paduan-Filho, N. F. Oliveira Jr., S. Haas, A. Steppke, C. F. Miclea, F. Weickert, R. Movshovich, E.-D. Mun, V. S. Zapf, and T. Roscilde, *ibid.* **489**, 379 (2012); D. Hönig, S. Zhao, M. Månsson, T. Yankova, E. Ressouche, C. Niedermayer, M. Laver, S. N. Gvasaliya, and A. Zheludev, Phys. Rev. B **85**, 100410(R) (2012); S. Krinner, D. Stadler, J. Meineke, J.-P. Brantut, and T. Esslinger, arXiv: 1311.5174 [quant-ph]; K. R. A. Hazzard, B. Gadway, M. Foss-Feig, B. Yan, S. A. Moses, J. P. Covey, N. Y. Yao, M. D. Lukin, J. Ye, D. S. Jin, and A. M. Rey, arXiv: 1402.2354 [quant-ph], and references therein.
- [25] S. R. White, Phys. Rev. Lett. **69**, 2863 (1992); Phys. Rev. B **48**, 10345 (1993); U. Schollwöck, Rev. Mod. Phys. **77**, 259 (2005); G. De Chiara, M. Rizzi, D. Rossini, and S. Montangero, J. Comput. Theor. Nanosci. **5**, 1277 (2008).
- [26] A. R. Calderbank and P. W. Shor, Phys. Rev. A, **54**, 1098 (1996); A. M. Steane, Proc. R. Soc. London A, **452**, 2551 (1996).
- [27] W. Dür, G. Vidal, and J. I. Cirac, Phys. Rev. A **62**, 062314 (2000).
- [28] W. Dür, Phys. Rev. Lett. **87**, 230402 (2001); D. Kaszlikowski, L. C. Kwek, J. Chen, and C. h. Oh, Phys. Rev. A **66**, 052309 (2002); A. Sen(De), U. Sen, and M. Żukowski, *ibid.* **66**, 062318 (2002); R. Augusiak and P. Horodecki, *ibid.* **74**, 010305 (2006); T. Vértesi and N. Brunner, Phys. Rev. Lett. **108**, 030403 (2012). C.f. T. Vértesi and N. Brunner, arXiv:1405.4502 [quant-ph]; T. Moroder, O. Gittsovich, M. Huber, and O. Gühne, arXiv:1405.0262 [quant-ph].
- [29] H. Bethe, Z. Phys. **71**, 205 (1931).
- [30] J. T. Karvonen, L. J. Taskinen, and I. J. Maasilta, Phys. Rev. B **72**, 012302 (2005); J. Salafranca and L. Brey, *ibid.* **73**, 214404 (2006); H. C. Hsu, W. L. Lee, J.-Y. Lin, H. L. Liu, and F. C. Chou, *ibid.* **81**, 212407 (2010); T. Berlijn, D. Volja, and W. Ku, Phys. Rev. Lett. **106**, 077005 (2011); B. Jaworowski, P. Potasz, and A. Wojs, Superlattices and Microstructures **64**, 44 (2013), and references therein.
- [31] E. Lieb, T. Schultz, and D. Mattis, Ann. Phys. (N.Y.) **16**, 407 (1961); E. Barouch, B. M. McCoy, and M. Dresden, Phys. Rev. A **2**, 1075 (1970); E. Barouch and B. M. McCoy, *ibid.* **3**, 786 (1971).
- [32] S. Hill and W. K. Wootters, Phys. Rev. Lett. **78**, 5022 (1997); W. K. Wootters, *ibid.* **80**, 2245 (1998).
- [33] A. Sen(De) and U. Sen, Phys. Rev. A **81**, 012308 (2010); A. Sen(De) and U. Sen, arXiv:1002.1253 [quant-ph].
- [34] A. Shimony, Ann. N.Y. Acad. Sci. **755**, 675 (1995); H. Barnum and N. Linden, J. Phys. A **34**, 6787 (2001); T.-C. Wei and P.M. Goldbart, Phys. Rev. A **68**, 042307 (2003); M. Balsone, F. Dell'Anno, S. De Siena, and F. Illuminati, *ibid.* **77**, 062304 (2008).